Thrombus Imaging with Indium-111 and Iodine-131-Labeled Fibrin-Specific Monoclonal Antibody and Its F(ab')$_2$ and Fab Fragments

Scott F. Rosebrough, Zachary D. Grossman, John G. McAfee, Bohdan J. Kudryk, Gopal Subramanian, Catherine A. Ritter-Hrncirik, Larry S. Witanowski, Gwen Tillapaugh-Fay, Enrique Urrutia, and Chris Zapf-Longo

Divisions of Nuclear Medicine and Radiological Sciences, Department of Radiology, SUNY Health Science Center, Syracuse, New York

We have previously reported successful imaging of fresh (2–4 hr old) and aged (1–5 days old) canine thrombi with ^{131}I-labeled intact monoclonal antibody (MAb) specific for fibrin. We now report thrombus imaging with ^{131}I-labeled F(ab')$_2$ and Fab and ^{111}In-labeled intact MAb, F(ab')$_2$, and Fab. Indium-111-labeled F(ab')$_2$ proved to be the best imaging agent due to less nonspecific binding in the liver than whole IgG. Image quality was improved by the higher administered dose permissible with ^{111}In and its better physical characteristics for imaging, compared to ^{131}I. Immunofluorescence of fresh human histologic sections showed intact MAb and F(ab')$_2$ binding to thrombi, pulmonary emboli, and atherosclerotic plaques, strengthening the feasibility of clinical thrombus imaging.

J Nucl Med 29:1212–1222, 1988

Radioimmunoimaging of fresh and aged canine venous thrombi with iodine-131-(^{131}I) labeled fibrin-specific MAb T2Gls has proven successful (*1,2*). The antigenic site is between amino acids 15–22 on the beta-chain of human fibrin (*3*). Because this amino-terminal region is identical in man and dog, we have been able to evaluate it for thrombus imaging in the dog. Fortunately, this MAb does not react with intact fibrinogen, circulating cells, or vascular endothelium.

Radioimmunoimaging has been directed primarily at cancer detection (*4,5*). For success, sufficient radiolabeled antibody must leave the vascular space to bind the antigen and provide contrast between the radioactivity in the target compared to other organs and background. To improve target/nontarget ratios, many investigators have used F(ab')$_2$ and Fab (*6–8*). Theoretically, these smaller molecular weight fragments should clear from the blood faster than intact IgG and enter into the interstitial fluid in contact with tumor cells. With thrombus imaging, on the other hand, the radiolabeled MAb has direct access to the intravascular lesion and the target antigen, fibrin. Moreover, the amount of antigen is far greater than that of most antigens of malignant cells, allowing ample binding for the radiolabeled antibody.

In attempting to improve image quality for thrombus detection, we investigated ^{131}I-labeled F(ab')$_2$ and Fab and indium-111-(^{111}In) labeled MAb, F(ab')$_2$, and Fab. The concentration of fibrin-specific MAb or fragments, in the thrombus, whole blood, and normal muscle was compared to that of indium-125-(^{125}I) labeled control nonspecific polyclonal murine IgG, F(ab')$_2$, or Fab.

Received Feb. 23, 1987; revision accepted Feb. 11, 1988.

For reprints contact: Scott F. Rosebrough, PhD, Divs. of Nuclear Medicine and Radiological Sciences, Dept. of Radiology, SUNY Health Science Center, Syracuse, New York.

MATERIALS AND METHODS

Thrombus Production

Mongrel dogs weighing 17–27 kg (mean 22 kg) were anesthetized with pentobarbital (30 mg/kg). A femoral venous thrombus was produced by percutaneous transcatheter placement of a Gianturco coil (*9*). The venipuncture site for catheter introduction was the jugular vein, so that the resultant trauma was remote from the imaging site, and the thrombus-containing lower limb could be compared with the contralateral normal side. Eight-millimeter coils were inserted through

a 5-French polyethylene catheter (Cook, Bedford, MA) under fluoroscopic control. Coil position was confirmed by fluoroscopy and radiography.

F(ab')$_2$ and Fab Production and Purification

Anti-fibrin MAb was produced and supplied by Dr. Kudryk at the New York Blood Center (*3*). To produce F(ab')$_2$ fragments, MAb and control antibody were digested overnight with a 1/30 w/w ratio of pepsin/IgG at 37°C. The antibodies were originally in 0.05*M* Tris/0.15*M* NaCl buffer (pH 7.0). Prior to digestion, the pH was lowered to 4.0 by adding 1/9 (v/v) of 1*M* NaAc buffer (pH 4.0). Samples were analyzed before and after pepsin digestion by 7.5% SDS-PAGE (Fig. 1B). The digestion of IgG into its F(ab')$_2$ fragment was evident by reduction in molecular weight and lack of immunoprecipitation when tested against goat anti-mouse Fc. However, immunodiffusion was positive when tested against goat anti-mouse whole IgG. To purify the F(ab')$_2$ fragments, the sample was passed through an S-12 FPLC gel filtration column (Pharmacia Inc., Piscataway, NJ) and the appropriate peak collected (Fig. 1A). Fab fragments were produced by digesting MAb with a 1/100 (w/w) ratio of papain to IgG in .2M PBS (pH 7.0) containing 4 mm EDTA and 0.02*M* cysteine overnight at 37°C.

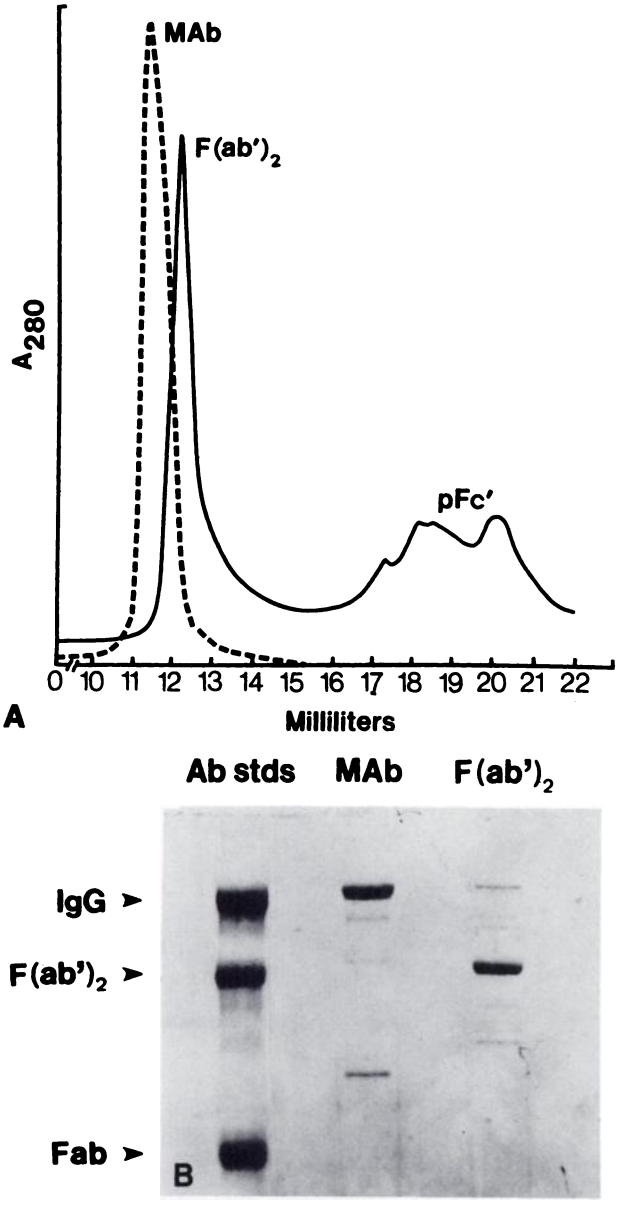

FIGURE 1
Purification and analysis of F(ab')$_2$ fragments by FPLC, compared with whole MAb and pFc' after pepsin digestion (A). SDS polyacrylamide gel electrophoresis of MAb, F(ab')$_2$ compared with mouse Ab standards (B).

Blood was drawn at 5, 10, 20, 30, 45, and 60 min, and at 2, 3, 4, 24, and 48 hr after antibody injection. Urine was collected by an indwelling catheter from 0–4 hr. At 48 hr the dogs were killed and the activity of ^{131}I- or ^{111}In-labeled fibrin-specific MAb (or fragments) and ^{125}I control nonspecific murine IgG (or fragments) was measured in the thrombus, whole blood and normal muscle; the activity was expressed as "% of injected dose per gram of tissue".

The activity in major organs was expressed as % dose/organ; it was assumed that the blood volume was 8% of the body weight, skeletal muscle 54.45%, and red marrow 2.14%.

For preliminary estimates of biologic half-lives and radiation doses, one dog was given 1 mCi of ^{111}In specific F(ab')$_2$ intravenously. For in vivo radioassay at 1, 2, 4, 6, and 8 hr, and 1, 2, 6, and 8 days, total-body counting was performed with an 8 in. × 2 in. sodium iodide (T1) crystal detector at a detector-skin distance of 49 cm. Liver and renal activity were quantitated at the same intervals by camera-computer techniques using a medium-energy, parallel hole collimator and areas of interest, in comparison with an appropriate organ phantom counted with the same geometry.

Immunohistochemistry

Postmortem human sections of all major organs, atheromatous thrombotic plaques and postmortem clots were snap frozen on gelatin coated slides for incubation with fibrin-specific MAb [or F(ab')$_2$] or control mouse IgG [or F(ab')$_2$]. Samples were then incubated with secondary anti-mouse IgG fluorescein conjugate. Both incubation times were 30 min, followed by three washes with phosphate buffered saline. Tissue sections 4 μm thick were mounted on gelatin-coated slides and examined by epi-illumination fluorescence (*13*). Preparative isoelectric focusing (PIEF) was used to separate Fc fragments from Fab fragments (*10*). Fab fragments focused at pH 7.0–8.0 and the Fc, much lower, at pH 4.9–5.6, as evident by immunodiffusion analysis of each PIEF fraction.

Antibody Labeling

MAb, F(ab')$_2$, or Fab were purified and labeled with ^{131}I as previously described (*1,2*). For labeling with ^{111}In, 0.15 mg of these purified materials were added to 0.35 ml of 0.42*M* HEPES buffer (pH 7.4) and mixed with 3 mg of solid diethylenetriaminepentaacetic acid (DTPA) cyclic dianhydride (*11*). On incubation overnight in a refrigerator, the DTPA became covalently linked to the protein amino groups. Residual-free DTPA was removed by centrifugal Centricon-30 filtration. Indium-111 citrate was prepared from commercial carrier-free indium chloride in 0.05*M* HCl by adding an equal volume of 0.1*M* sodium citrate solution (pH 6). The intact MAb, F(ab')$_2$, or Fab fragments conjugated with DTPA in 0.1 to 0.2 ml of saline were mixed with 2–11 mCi of [^{111}In]citrate and incubated overnight in a refrigerator. The labeling efficiency

averaged 37%. Labeled protein was purified by centrifugal C-30 Centricon ultrafiltration and collected in 0.5 to 2 ml of isotonic saline. The final concentration ranged from 4–20 mCi/mg protein. By gel filtration chromatography with a P6DG gel column, more than 96% of the radioactivity in the final product was protein bound.

Immunoreactivity Analysis

The immunoreactivity of the ^{131}I- and ^{111}In-labeled F(ab')$_2$ was measured by affinity chromatography in which human fibrin was covalently bound to sepharose 6MB (Pharmacia). Human fibrinogen (Sigma Chemical Company, St. Louis, MO) was coupled to CNBr-activated sepharose 6MB overnight at room temperature following Pharmacia's protocol. Fibrinogen concentration was estimated by uv absorbance at 280 nm. The sample was read in 0.2N NaOH/5*M* urea using an extinction coefficient of 16.7 for a 1% solution (*12*). 21.73 of the 25.7 mg fibrinogen were added bound to 3 g of swollen sepharose. After washing the gel with 0.05*M* Tris/0.15*M* NaCl, pH 7.0, and blocking any unreactive groups with 0.2*M* glycine in coupling buffer, the 14 ml gel slurry was incubated with 40 units of thrombin (Sigma) in Tris/saline for 3 hr at room temperature. The fibrin-sepharose slurry was brought up to 66 ml with 0.1% BSA Tris/saline buffer containing 130 units aprotinin (Sigma).

Thirty nanograms of ^{131}I or ^{111}In F(ab')$_2$ were mixed with 50 μl of the fibrin-sepharose in 0.25 ml of 0.1% BSA Tris/saline buffer overnight at room temperature in 0.5 ml microcentrifuge tubes. The total amount of radioactivity per tube was determined by a gamma counter. The gel was centrifuged, decanted, and washed with 0.3 ml of 0.1% BSA in Tris/saline and percentage bound radioactivity was determined by counting the pellet after centrifugation.

Blood Clearance and Biodistribution

Each dog was injected intravenously in a forelimb with similar quantities (10–40 μg) of fibrin-specific antibody (or fragment) and control antibody (or fragment) within the first 3 hr of thrombus induction. Control antibody (or fragment) was labeled with 50 to 75 μCi of ^{125}I. Fibrin-specific MAb (or fragment) was labeled with ~175 μCi of ^{131}I or 300 μCi of ^{111}In.

Anterior images of the lower pelvis and legs, abdomen, and chest were obtained immediately and at 2, 4, 20, and 48 hr. After the 48-hr image, 50 cc of Renografin-60 were hand injected into a dorsal vein of the foot to obtain a venogram for comparison.

RESULTS

Immunoreactivity

Immunoreactivity of ^{131}I and ^{111}In F(ab')$_2$'s, prepared and labeled identically to those used in vivo, was measured by affinity chromatography using fibrin-coated sepharose. (Immunoreactivity of the F(ab')$_2$'s actually used in dog studies was not measured). To test the consistency of DTPA coupling, three 0.15-mg samples were incubated overnight with DTPA, labeled with 2 mCi of ^{111}In and tested for immunoreactivity. The binding of the ^{111}In F(ab')$_2$ samples was 79.8 ± 1.7, 81.2 ± 1.8, and 83.7 ± 6.8% (n = 3 per sample). Since the differences were not significant, the data were averaged (81.6 ± 4.0). Iodine-131 F(ab')$_2$ had similar binding of 85.8 ± 1.1. Nonspecific binding was negligible as indicated by less than 5% ^{125}I control F(ab')$_2$ binding (Fig. 2).

IMAGES

Composite venograms and nuclear images of ^{131}I F(ab')$_2$, ^{111}In MAb, ^{111}In F(ab')$_2$, appear in Figure 3. Each venogram reveals a "filling defect" representing a thrombus surrounding the Gianturco coil. Nuclear images were clearly positive 20 and 48 hr after antibody injection in all dogs injected with MAb or F(ab')$_2$. However, in dogs injected with ^{111}In- or ^{131}I-labeled Fab, images were negative.

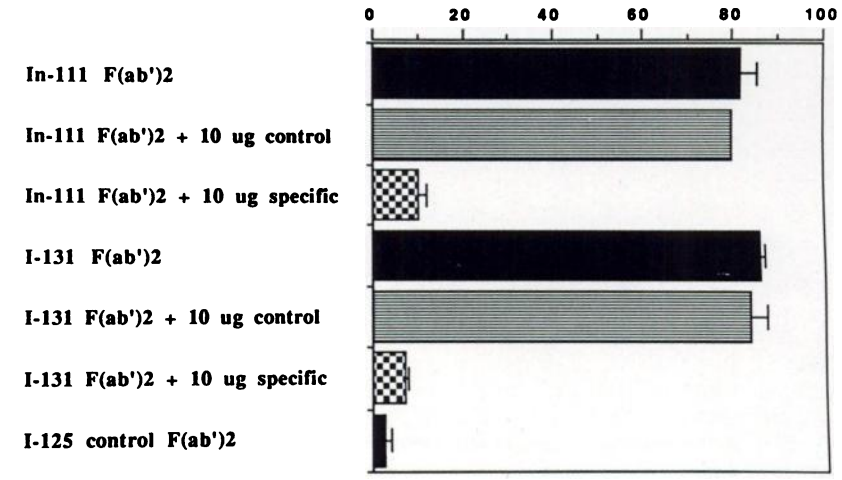

FIGURE 2
Immunoreactivity of ^{131}I and ^{111}In F(ab')$_2$ measured by affinity chromatography using fibrin coated sepharose. Iodine-131 (n = 6) and ^{111}In (n = 9) specific F(ab')$_2$ bound to fibrin-sepharose greater than 82% in the presence (n = 3) or absence of 10 μg control F(ab')$_2$. However, when 10 μg of cold specific F(ab')$_2$ were added (n = 3) the amount of bound radiolabeled F(ab')$_2$ was significantly reduced, indicating specific competition between radio-labeled and cold F(ab')$_2$ for the antigen. Iodine-125 Fab nonspecific binding was <5%.

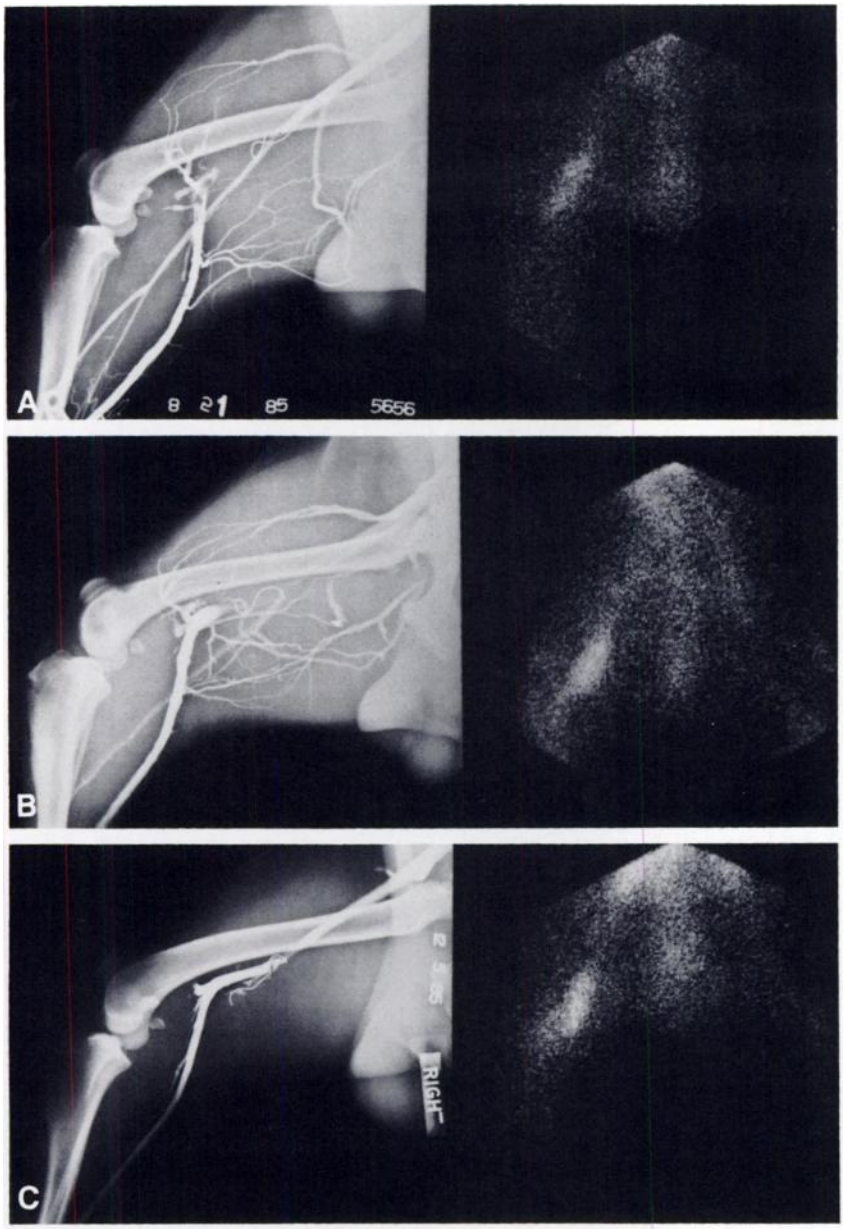

FIGURE 3
Venograms (left) and images (right) of right lower limbs of dogs 20 hr after induction of femoral venous thrombi with Gianturco coils. (A) ^{131}I F(ab′)$_2$ (B) ^{111}In whole MAb (C) ^{111}In F(ab′)$_2$.

Radiobioassay and Blood Clearance

The thrombus concentration of radiolabeled MAb and specific F(ab′)$_2$ was similar in all dogs (Tables 1 and 2). Target-to-background ratios, expressed as clot/blood and clot/muscle, for the fibrin-specific MAb and its F(ab′)$_2$, ranged from 9–16 and 174–317, respectively. These ratios for control IgG and control F(ab′)$_2$ ranged from 0.8–1.1 (clot/blood) and 11–15 (clot/muscle). Thrombus concentrations of the fibrin-specific Fab fragments were much less than the whole IgG or F(ab′)$_2$ fragment (Tables 1 and 2).

Multiexponential analyses of the blood levels during the first 48 hr showed satisfactory curve fitting (coefficient of determination $R^2 > 0.999$) with only two components for whole IgG, F(ab′)$_2$, and ^{131}I Fab (Table 3, Figure 4A,B,C). Indium-111 Fab clearance was best fitted by three exponentials, with a very short component with a t½ of 0.12 hr and an intercept of ~61%. The plasma disappearance curves were identical to those of whole blood, indicating complete lack of diffusion into blood cells. Whole MAb labeled with ^{131}I had the slowest clearance. The clearances of ^{111}In MAb and specific ^{131}I F(ab′)$_2$ were similar. Moreover, the clearance of ^{111}In F(ab′)$_2$ was not significantly faster than ^{111}In MAb. The clearance of the radioiodinated Fab was relatively fast, and that of ^{111}In specific Fab very rapid (Fig. 4C), with large "faster" components.

Table 4 compares the 48-hr biodistributions of the specific IgG and its fragments in the major organs. The blood level of ^{131}I specific IgG is highest, and those of ^{111}In IgG, ^{131}I, and ^{111}In F(ab′)$_2$ are similar. The concentration of ^{131}I in the unblocked thyroid is relatively

TABLE 1
Mean Activity (+1 s.d.) of ^{131}I Fibrin-Specific Mab, F(ab′)$_2$, or Fab and ^{125}I Control IgG, F(ab′)$_2$ or Fab in Dogs at 48 hr

	Whole IgG			F(ab′)$_2$			Fab		
	n = 3			n = 3			n = 3		
	Spec	Control	Spec/ Control	Spec	Control	Spec/ Control	Spec	Control	Spec/ Control
Blood*	0.029 ± 0.002	0.014 ± 0.001	2.1	0.018 ± 0.006	0.014 ± 0.004	1.2	0.0032 ± 0.0008	0.0038 ± 0.0010	0.8
Clot*	0.252 ± 0.130	0.017 ± 0.006	14.8	0.186 ± 0.051	0.011 ± 0.001	16.9	0.0281 ± 0.0024	0.0051 ± 0.0013	5.5
Muscle*	0.0011 ± 0.0002	0.0012 ± 0.0005	0.9	0.0011 ± 0.0002	0.0011 ± 0.0003	1.0	0.0004 ± 0.0001	0.0005 ± 0.0001	0.8
Clot/blood	8.6 ± 4.1	1.2 ± 0.3	7.2	10.9 ± 1.5	0.84 ± 0.19	13.0	9.2 ± 2.8	1.3 ± 0.17	7.1
Clot/muscle	238 ± 153	15 ± 7	15.9	174 ± 21	11 ± 3	15.8	74.3 ± 24.1	11.1 ± 3.3	6.7

* % dose/g.

TABLE 2

Mean Activity (+1 s.d.) of ^{111}In Fibrin-Specific Mab, F(ab′)$_2$, or Fab and ^{125}I Control IgG, F(ab′)$_2$ or Fab in Dogs at 48 hr

	Whole IgG			$F(ab')_2$			Fab			
	n = 3			n = 6			n = 3			
	Spec	Control	Spec/ control	Spec	Control	Spec/ control	Spec	Control	Spec/ control
Blood*	0.017 ± 0.006	0.023 ± 0.005	0.7	0.017 ± 0.003	0.014 ± 0.002	1.2	0.0005 ± 0.0002	0.0044 ± 0.0006	0.1
Clot*	0.259 ± 0.090	0.017 ± 0.001	15.2	0.252 ± 0.167	0.016 ± 0.006	15.8	0.0023 ± 0.0009	0.0049 ± 0.0004	0.5
Muscle*	0.0010 ± 0.0006	0.0014 ± 0.0006	0.7	0.0010 ± 0.0003	0.0016 ± 0.0009	0.6	0.0001 ± 0.0000	0.0005 ± 0.0001	0.2
Clot/blood	16.0 ± 4.4	0.76 ± 0.13	21.0	15.2 ± 11	1.1 ± 0.3	13.8	5.0 ± 2.0	1.1 ± 0.1	4.5
Clot/muscle	317 ± 117	13 ± 4.5	24.4	276 ± 186	11 ± 4.0	25.1	35.3 ± 4.2	9.2 ± 0.5	3.8

* % dose/g.

TABLE 3
Biexponential Analysis of Blood Clearance Curves*

		n	Slower component: Intercept % dose in blood vol	Slower component: T-½ hr	Faster component: Intercept % dose in blood vol	Faster component: T-½ hr
IgG	Iodine-131 spec	12	82	50	16	1.4
	Iodine-125 non-spec	12	68	32	31	0.69
	Indium-111 spec	3	76	33	24	1.7
	Iodine-125 non-spec	3	75	46	25	2.2
$F(ab')_2$	Iodine-131 spec	3	80	30	20	2.5
	Iodine-125 non-spec	3	74	29	23	2.2
	Indium-111 spec	6	85	28	15	0.86
	Iodine-125 non-spec	6	82	24	18	0.74
Fab	Iodine-131 spec	3	38	13	47	0.71
	Iodine-125 non-spec	3	37	15	55	0.67
	Indium-111 spec†	3	5.5	16	13	0.65
	Iodine-125 non-spec	3	25	30	62	1.0

* $R^2 > 0.999$.
† Third ultrafast component t½ - ~0.12 hr.

low for all preparations. Indium-111 whole IgG reaches a high concentration in the liver. In contrast, ^{111}In $F(ab')_2$ has a lower liver uptake, but a higher renal uptake. The marrow concentrations of ^{111}In IgG and $F(ab')_2$ are low, and similar to that of ^{131}I IgG. The residual organ activity of ^{131}I Fab is low, and very low for ^{111}In Fab. The available data on urinary excretion during the first 4 hr are listed in Table 4. From these data and the integrated plasma levels during the first 4 hr, renal clearances were estimated according to the method of Rehling et al. (*14*). The renal clearance of ^{111}In IgG was negligible (~0.1 ml/min). The clearance of ^{131}I Fab was 1.24 ml/min, and 30 ml/min for ^{111}In Fab. By column chromatography, most of this urinary ^{111}In activity was free [^{111}In]DTPA complex. The renal clearance of ^{111}In $F(ab')_2$ estimated by the uv/P method was considered invalid because of its accumulation in the renal cortex.

Radiation dose estimates from ^{111}In $F(ab')_2$ in standard man, based on the canine biodistribution data and calculated from MIRD "S" factors are listed in Table 5. The blood radiation dose estimates are based on the method of Cloutier et al. (*15*). In the left column, no biologic excretion was assumed; in the right column the biologic excretion in man and dog was assumed to be identical. The total-body activity (from total-body counting) had two exponential components—82% with a biologic half-time of 20 days, and 18%, 9 hr (Fig. 5). The liver was assumed to have an instantaneous uptake of 20.6% of the administered activity and a biologic half-life of 7 days. The two kidneys reached peak activity of 12% at 24 hr—7.5% with a biologic half-time of 20 days and 4.5%, 1 day; the initial biologic uptake half-time was 4 hr. Probably the real radiation dose estimates in man will prove to be between the two sets of estimated values, because biologic half-times usually are longer in man than in the dog. In either of the two radiation dose estimates, the organ receiving the largest dose is the kidney, rather than the liver. The renal accumulation is seen on delayed images (Fig. 6). The biologically critical organ is probably the red marrow, and its radiation dose appears low.

Human Section Histochemistry

Fibrin-specific MAb fragments showed no cross-reactivity to normal human tissues. However, binding of whole MAb or control IgG to cells of the macrophage line was observed (e.g., Kupffer cells in the liver, spleen and lymph node macrophages) (Fig. 7). This binding was not observed with either fibrin-specific $F(ab')_2$ fragment or control $F(ab')_2$ fragment. Positive reactions with fibrin-specific MAb and $F(ab')_2$ fragment were seen in clots, fibrinous adhesions, pulmonary emboli and thrombi adherent to ulcerated atherosclerotic plaques. Control IgG or $F(ab')_2$ fragment had no such binding.

DISCUSSION

Many other radiolabeled agents have been tried for imaging thrombi (*16*) including highly iodinated fibrinogen, soluble fibrin, plasmin, plasminogen, streptokinase, urokinase, and fibrin fragment E, but these have not achieved widespread clinical acceptance. Indium-111-labeled platelets and radioiodinated fibrinogen have been used in many clinical studies. In a comparison of these two agents in dogs (*17*), labeled platelets proved superior to fibrinogen for fresh thrombi, but offered no advantage for thrombi over 24 hr old. At 48 hr after thrombus induction and 24 hr after injection, the mean thrombus/blood concentration ratios were 1.8:1 for labeled platelets and 2.2:1 for fibrinogen. In comparison, this ratio was 15–16:1 for our ^{111}In-labeled MAb or $F(ab')_2$ fragments.

We found that relatively large cyclic DTPA anhydride/MAb molar ratios were required for these experiments. The conditions were different than in published methods in which milligram quantities of MAb were

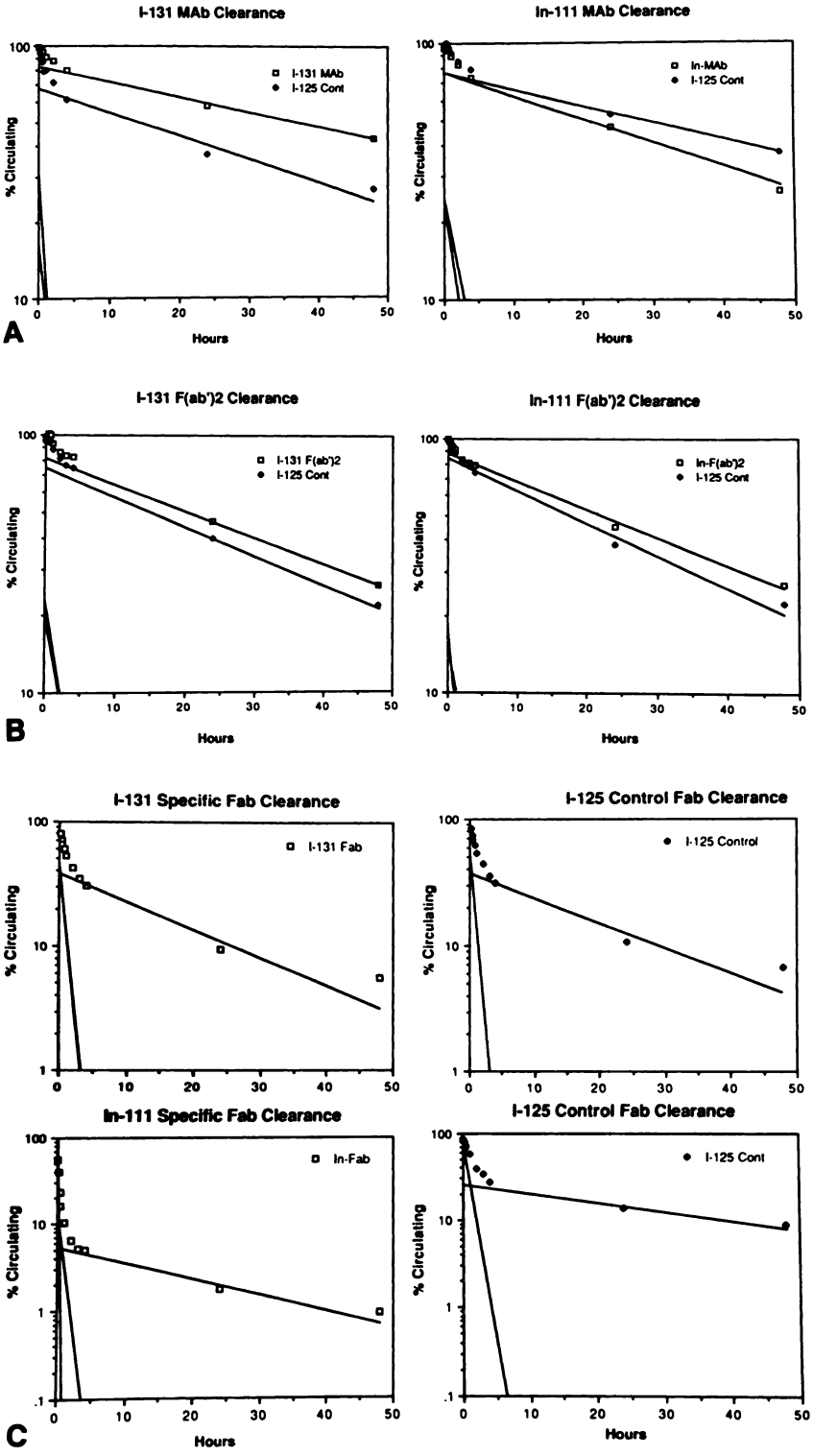

FIGURE 4
Blood clearances. A: Whole MAb in dogs over 48 hr (corrected for decay) compared with nonspecific ^{125}I control murine IgG. Lines show exponential components. B: Fibrin-specific F(ab')$_2$ compared with ^{125}I nonspecific F(ab')$_2$. C: Iodine-131 (upper row) and ^{111}In (lower row) fibrin-specific compared with ^{125}I nonspecific Fab.

coupled. The variables involved in the coupling reaction other than the molar ratio include (a) each MAb couples differently (b) pH, (c) type of buffer, (d) molarity of the buffer, (e) amount of each reagent, and (f) reaction volume (*11*). With a relatively small quantity of one MAb (300 μg/ml) and a molar ratio of 50:1 at pH 8.4, Paik (*11*) obtained only 1.3 atoms of ^{111}In/Ab molecule. With a lower pH, coupling efficiency was even lower. We observed that coupling even smaller quantities of MAb (150 μg) was technically difficult. The coupling efficiency and subsequent ^{111}In labeling yield fell precipitously with this small quantity and the high molar ratios were necessary because of the loss from spontaneous hydrolysis of the cyclic dianhydride to DTPA. Other conditions (HEPES buffer 0.44*M* at pH 7.4) were unique to our experiments. Despite the high molar

TABLE 4
Biodistribution of Specific Anti-Fibrin MAb and Its Fragments in Dogs: Mean % Dose/Organ

	Iodine-131			Indium-111		
	IgG	F(ab')$_2$	Fab	IgG	F(ab')$_2$	Fab
0-4 urine	—	—	13	2.9	3.1	74
48 hr						
Blood	46	26	5.6	25	27	0.93
Thyroid	1.5	2.3	3.1	0.004	0.005	0.001
Liver	6	—	1.4	45	21	3.0
Spleen	—	—	0.49	1.3	2.4	0.24
Two kidneys	—	1.0	0.29	1.3	9.6	0.39
Muscle	12	11	4.8	9.7	9.6	0.74
Red marrow	2.2	—	0.32	2.3	2.1	0.14

ratios, ^{111}In F(ab')$_2$ retained a high percentage of immunoreactivity (80–84%) and was equivalent to that of ^{131}I F(ab')$_2$.

In all canine experiments to date, the in vivo thrombus concentration of labeled monoclonal antibody T2G1 or its F(ab')$_2$ was clearly superior to simultaneously injected nonspecific murine IgG or fragments. Iodine-131 specific MAb had a relatively slow blood clearance and low thyroid uptake, suggesting that significant dehalogenation in vivo did not occur, unlike certain tumor-specific MAbs. The blood clearance of ^{111}In specific MAb was somewhat faster than that of ^{131}I MAb, due to marked uptake by the liver. Immunofluorescence showed binding of unlabeled specific MAb and control IgG by Kupffer cells and no such binding by F(ab')$_2$ fragments. Labeled specific Fab fragments (mol wt ~50,000) proved unsatisfactory for thrombus imaging probably because of their rapid blood clearance. The renal clearance of ^{111}In Fab (30 ml/min) approached that of [^{111}In]DTPA in the dog (71 ml/min), calculated from previous data (*18*), by the method of Rehling et al. (*14*). However, the recovery of free [^{111}In]DTPA complex in addition to some protein-bound activity in the urine from ^{111}In Fab administration suggested that this conjugate was unstable in vivo.

We consider ^{111}In specific F(ab')$_2$ the agent of choice

TABLE 5
Radiation Dose Estimates in Man Extrapolated from Dog Data; ^{111}In Anti-Fibrin F(ab')$_2$

	Biologic excretion (rad/mCi)	
	No	Yes
Total body	0.57	0.36
Liver	3.0	2.1
Spleen	2.9	1.9
Kidneys	5.6	4.1
Red Marrow	0.82	0.52
Blood	1.43	0.37
Ovaries	0.67	0.41
Testes	0.49	0.29

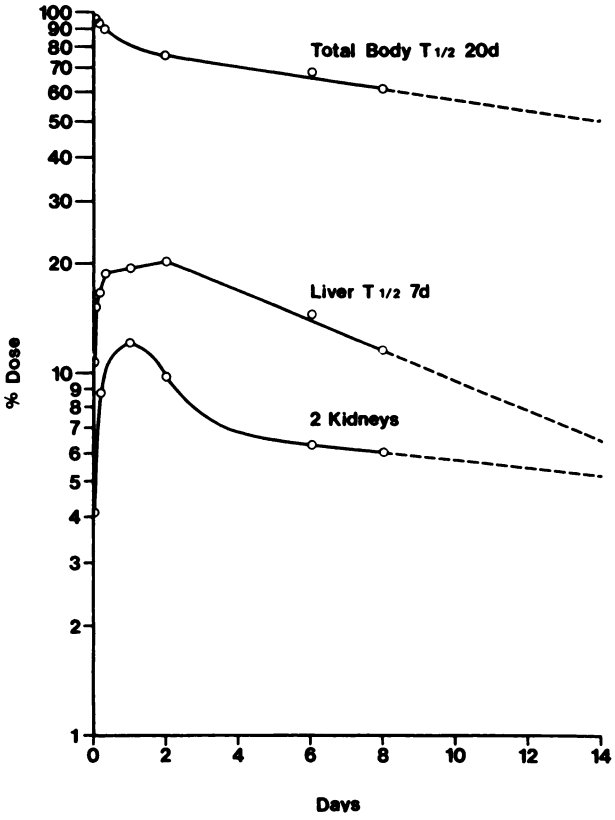

FIGURE 5
Changes in activity for ^{111}In F(ab')$_2$ in total body, liver, and kidneys over 8 days (corrected for decay).

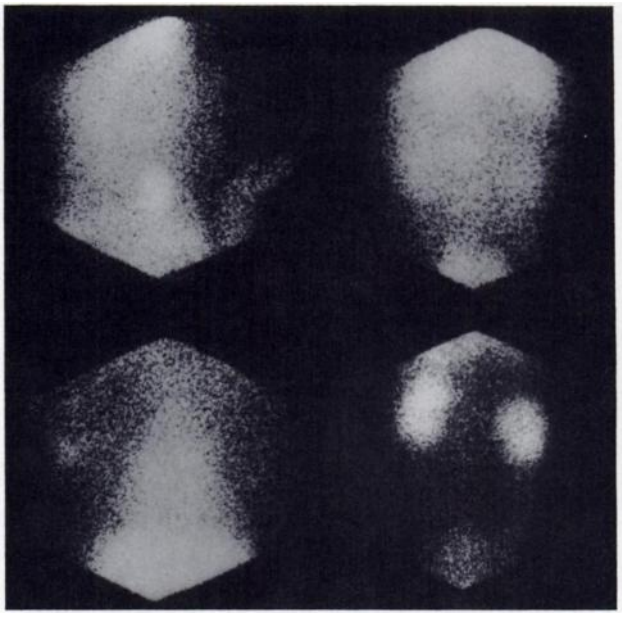

FIGURE 6
Images after injection of ^{111}In F(ab')$_2$. (Left upper) localized uptake in the left neck at 40 hr at the site of the catheter insertion. (Left lower) persistent cardiovascular blood-pool and hepatic activity at 40 hr. (Right upper) bladder and faint renal activity at 2 hr. (Right lower) higher renal activity and lower diffuse abdominal activity at 40 hr.

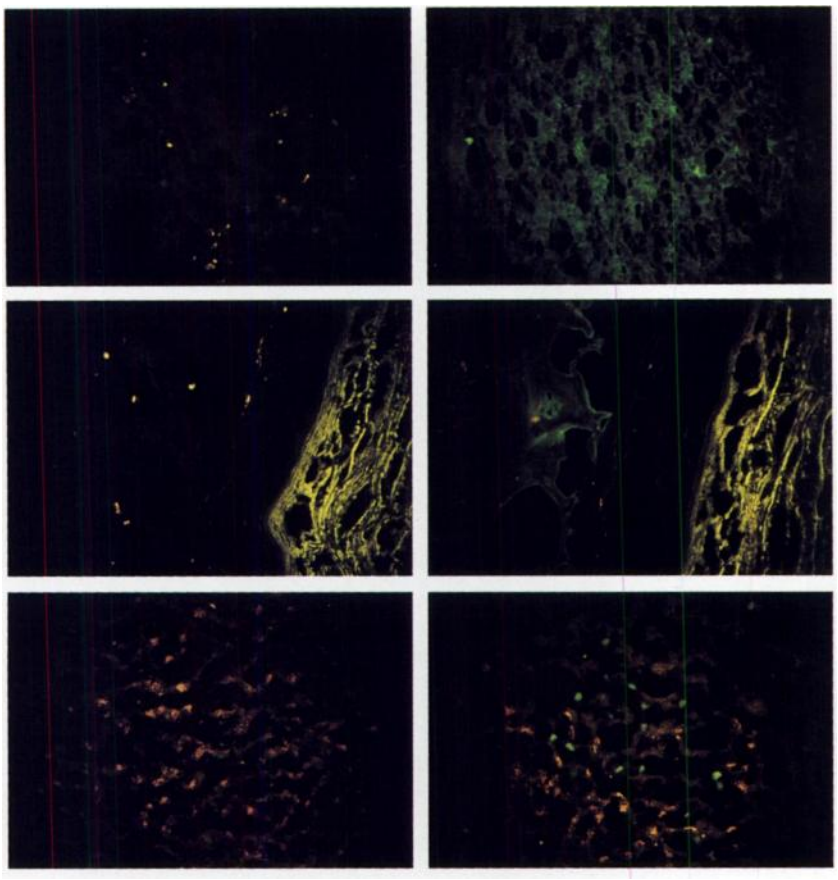

FIGURE 7
Indirect immunofluorescence of postmortem frozen human tissue sections. (Top row) Thrombus. Fluorescein indirectly-labeled IgG (green) is more intense for the MAb (right) than for nonspecific IgG (left). Autofluorescent elastin appears yellow. (Middle row) Pulmonary embolus. MAb (right) stains more intensely than nonspecific IgG (left). Elastin network in capillary wall. (Bottom row) Liver. Specific $F(ab')_2$ (left) shows no green fluorescence. Specific intact MAb (right) shows spots of green fluorescence on Kupffer cells.

for thrombus detection in future human trials. The gamma emissions of ^{111}In are superior to those of ^{131}I for camera imaging, and the resultant radiation dose from ^{111}In is less, because of its shorter physical half-life and lack of beta emissions. Clinical imaging frequently would be an emergency procedure, requiring a continuing supply of radionuclide. Hence, we considered ^{111}In preferable to "pure" ^{123}I for this application, because the difference in physical half-lives (67 hr versus 12 hr, respectively) would favor the former economically. Although the blood levels and thrombus concentrations of specific $F(ab')_2$ and IgG labeled with ^{111}In are similar, the former has immunologic advantages. The production of human anti-murine antibodies may be less. Moreover, successful thrombus imaging was achieved with smaller amounts of $F(ab')_2$ (2 μg/kg) than commonly used for imaging neoplasms. Nonspecific binding of whole IgG to Fc receptors of leukocytes or fixed macrophages of the liver or spleen is eliminated with $F(ab')_2$ fragments. Consequently, the very high liver concentration of ^{111}In IgG is avoided with ^{111}In $F(ab')_2$ fragments. The progressive renal uptake of ^{111}In from these labeled fragments over 24 hr, with low urinary excretion of radioactivity suggests that they are readily cleaved in vivo to smaller protein and polypeptide fragments which accumulate in renal tubular cells for further catabolic breakdown, similar to the fate of other low molecular weight proteins. The low concentration of ^{111}In in the marrow up to 48 hr indicates that no significant transchelation to plasma transferrin occurs in vivo. Some of the results to be obtained in initial human trials may not agree with the above findings due to species differences.

ACKNOWLEDGMENTS

This research was supported by Grant No. HL 24230-06 awarded by the National Heart, Lung and Blood Institute, DHHS and by a research fellowship to Scott F. Rosebrough from the RSNA Research and Education Fund.

REFERENCES

1. Rosebrough SF, Kudryk B, Grossman ZD, et al. Radioimmunoimaging of venous thrombi using iodine-131 monoclonal antibody. *Radiology* 1985; 156:515–517.
2. Rosebrough SF, Grossman ZD, McAfee JG, et al. Aged venous thrombi: radioimmunoimaging with fibrin-specific monoclonal antibody. *Radiology* 1987; 162:575–577.
3. Kudryk B, Rohoza A, Aladi M, et al. Specificity of a monoclonal antibody for the NH_2-terminal region of fibrin. *Mol Immunol* 1984; 21:89–94.

4. Larson SM, Carrasquillo JA, Reynolds JC. Radioimmunodetection and radioimmunotherapy. *Cancer Invest* 1984; 265:363–381.
5. Bradwell AR, Fairweather DS, Dykes PW, et al. Limiting factors in the localization of tumours with radiolabeled antibodies. *Immunology Today* 1985; 6:163–170.
6. Wahl RL, Parker CW, Philpott GW. Improved radioimaging and tumor localization with monoclonal $F(ab')_2$. *J Nucl Med* 1982; 24:316–325.
7. Mach JP, Chatal JF, Lumbroso JD, et al. Tumor localization in patients by radiolabeled monoclonal antibodies against colon carcinoma. *Cancer Res* 1983; 43:5593–5600.
8. Houston LL, Nowinski RC, Bernstein ID. Specific in vivo localization of monoclonal antibodies directed against the the 1.1 antigen. *J Immunol* 1980; 125:837–843.
9. Chuang VP, Wallace S, Gianturco C. A new improved coil for tapered tip catheter for arterial occlusion. *Radiology* 1980; 135:507–509.
10. Rosebrough SF, Grossman ZD, McAfee JG. Purification of fibrin-specific monoclonal antibody from ascites fluid by preparative isoelectric focusing. *Immunol Lett* 1986; 12:147–151.
11. Paik CH, Ebbert MA, Murphy PR, et al. Factors influencing conjugation with antibodies by cyclic DTPA anhydride. *J Nucl Med* 1983; 24:1158–1163.
12. Mosesson MW, Alkjaersig N, Sweet B, et al. Human fibrinogen of relatively high solubility. Comparative biophysical, biochemical, and biological studies with fibrinogen of lower solubility. *Biochemistry* 1967; 6:3279–3287.
13. Bahmanyar S, Gajdusek DC, Satelo J, et al. Longitudinal spinal cord sections as substratum for anti-neurofilament antibody detection. *J Neur Sci* 1982; 53:85–90.
14. Rehling M, Moller ML, Thamdrop B, et al. Simultaneous measurement of renal clearance and plasma clearance of ^{99m}Tc-labelled diethylaminetriaminepenta-acetate, ^{51}Cr-labelled ethylenediaminetetraacetate and inulin in man. *Clin Sci* 1984; 66:613–619.
15. Cloutier RJ, Watson EE. Radiation dose from radioisotopes in the blood. In: Cloutier RJ, Edwards CL, Snyder WS, eds. *Medical radionuclides: radiation dose and effects.* Oak Ridge, TN: AEC Symposium Series 20, US Atomic Energy Commission, Division of Technical Information, 1970:325–346.
16. McAfee JG, Subramanian G. Fibrinogen and other thrombus-localizing agents. In: Freeman LM, ed. *Freeman and Johnson's Clinical Radionuclide Imaging*, 3rd Ed., Vol 1. New York: Grune & Stratton, Inc., 1984:156–158.
17. Knight LC, Primeau JL, Siegel BA, et al. Comparison of In-111-labeled platelets and iodinated fibrinogen for the detection of deep venous thrombosis. *J Nucl Med* 1978; 19:891–894.
18. McAfee JG, Gagne G, Atkins HL, et al. Biological distribution and excretion of ^{99m}Tc and ^{111}In labeled DTPA. *J Nucl Med* 1979; 20:1273–1278.